



Research Article

Particles Detection System with CR-39 Based on Deep Learning

Gal Amit ^{1,2}, **Idan Mosseri**,³ **Ofir Even-Hen** ¹, **Nadav Schneider** ³, **Elad Fisher** ^{3,4},
Hanan Datz ¹, **Eliahu Cohen** ², and **Noaz Nissim** ⁵

¹Radiation Safety Department, Soreq Nuclear Research Center, Yavne, Israel

²Faculty of Engineering and the Institute of Nanotechnology and Advanced Materials, Bar Ilan University, Ramat Gan 5290002, Israel

³Technology Division, Soreq Nuclear Research Center, Yavne, Israel

⁴Maritime Policy & Strategy Research Center (HMS), Hatter Department of Marine Technologies, University of Haifa, Haifa 3498838, Israel

⁵Applied Physics Department, Soreq Nuclear Research Center, Yavne, Israel

Correspondence should be addressed to Gal Amit; galam@soreq.gov.il

Received 10 May 2022; Accepted 14 June 2022; Published 30 June 2022

Academic Editor: Dimitri Batani

Copyright © 2022 Gal Amit et al. This is an open access article distributed under the Creative Commons Attribution License, which permits unrestricted use, distribution, and reproduction in any medium, provided the original work is properly cited.

We present a novel method that we call FAINE, fast artificial intelligence neutron detection system. FAINE automatically classifies tracks of fast neutrons on CR-39 detectors using a deep learning model. This method was demonstrated using a LANDAUER Neutrak® fast neutron dosimetry system, which is installed in the External Dosimetry Laboratory (EDL) at Soreq Nuclear Research Center (SNRC). In modern fast neutron dosimetry systems, after the preliminary stages of etching and imaging of the CR-39 detectors, the third stage uses various types of computer vision systems combined with a manual revision to count the CR-39 tracks and then convert them to a dose in mSv units. Our method enhances these modern systems by introducing an innovative algorithm, which uses deep learning to classify all CR-39 tracks as either real neutron tracks or any other sign such as dirt, scratches, or even cleaning remainders. This new algorithm makes the third stage of manual CR-39 tracks revision superfluous and provides a completely repeatable and accurate way of measuring either neutrons flux or dose. The experimental results show a total accuracy rate of 96.7% for the true positive tracks and true negative tracks detected by our new algorithm against the current method, which uses computer vision followed by manual revision. This algorithm is now in the process of calibration for both alpha-particles detection and fast neutron spectrometry classification and is expected to be very useful in analyzing results of proton-boron11 fusion experiments. Being fully automatic, the new algorithm will enhance the quality assurance and effectiveness of external dosimetry, will lower the uncertainty for the reported dose measurements, and might also enable lowering the system's detection threshold.

1. Introduction

Much interest in the aneutronic fusion reaction of proton-boron11 (p-B11) has risen lately due to the unexpectedly large amount of reactions obtained in several high intensity laser experiments (see, e.g., [1, 2]).

As the physical processes involved in the production of such excess of reactions are not yet fully understood and may even involve nonlinear processes such as the avalanche process [3, 4], intensive research programs are ongoing in many academic institutes and private companies [5–7].

Moreover, a high flux of highly energetic particles such as protons, heavy ions, and the desired fusion product of alpha-particles accompany the harsh plasma environment that characterizes laser-initiated p-B11 fusion experiments, making the analysis of such experiments a nontrivial task. The most common diagnostics in such experiments are solid state nuclear track detectors such as CR-39 [8, 9]. Although the CR-39 are very reliable for the measurement of the absolute alpha-particle flux, the analysis of the CR-39 passive detector involves a long and tedious process which includes chemical etching, a smart image analysis, and a manual

revision, thus limiting the accuracy and efficiency of the data analysis. For this reason, it is highly desirable to develop automatic software tools to carry out analysis for a large number of nuclear track detectors, hence enhancing the overall outputs of future p-B11 experiments at various laser facilities. That is the main goal behind our current research, which uses deep learning to automate the classification of neutron tracks on CR-39 detectors.

For fast neutron dosimetry, a CR-39 detector is added to a standard TLD card dosimeter. The CR-39 detector is composed of an organic polymer whose chemical name is polyallyl diglycol carbonate (PADC) and its chemical formula is $C_{12}H_{18}O_7$. It is suitable for neutron personal monitoring due to its high sensitivity to protons hit [10], which has been recognized some decades ago as a basic requirement for a fruitful neutron personal monitoring [11].

CR-39 detectors hold some important advantages for serving as neutron dosimeters, among them are their low fast neutron energy threshold, their insensitivity to photon and beta irradiation, their high sensitivity over a wide range of neutron energies [12, 13], and the low influence of environmental effects [14] on its response as well as low signal fading. Although other neutron detecting technologies, such as the bubble detector [15], may have advantages in sensitivity, angle, and energy response dependence, the CR-39 detector still remains the most versatile, easy to carry along with a TLD card, and cheapest neutron dosimeter alternative.

Nevertheless, the main drawback of CR-39 as a fast neutrons dosimeter is its ability to accurately measure high flux neutron fields due to the tedious task of counting the neutron tracks. Other challenges for the CR-39 are distinguishing between different neutron energies and distinguishing between neutrons and alpha-particles.

2. Materials and Methods

The External Dosimetry Lab (EDL) at Soreq Nuclear Research Center (SNRC) provides dosimetry services to all radiation workers around the country, most of them are monitored monthly for X-rays and gamma and beta radiation and some of them for both thermal and fast neutrons.

Since late 70's [16] and until recently, SNRC fast neutron dosimetry system has been an in-house system. In 2018, a new personal neutron dosimetry system, LANDAUER Neutrak[®] system, has been adopted at SNRC [17]. This system is designed to measure CR-39 detectors using a Zeiss microscope, which is coupled to a CCD camera and to a robotic arm that feeds the microscope's moving tray with plastic holders one at a time, each holder having six CR-39 detectors. The CR-39 detector dimensions are 9×19 mm.

After the EDL receives the CR-39 detectors from the customers, the first stage is the etching stage. The detectors are inserted for 15 hours into an etching bath filled with NaOH heated to 74°C at a concentration of 5.5 mol/l in order to enlarge the tracks size. After etching is finished, the CR-39 detectors are thoroughly rinsed to remove all etching residues, to achieve optimal optical reading conditions.

Following the rinsing stage, the second stage is imaging the etched CR-39 detectors using the CCD camera. Ten images of different areas of the CR-39 detector are taken for the fast neutron counting. The images are then analyzed by Landauer's computer vision analysis software. Afterwards, the EDL staff either adds undetected tracks (false negatives) or deletes detected tracks (false positives) using Landauer's data review SW, according to a set of rules adopted by the scientific lab team.

We developed for the first time to our knowledge a method that detects fast neutron tracks on CR-39 detectors, which is based on deep learning, and we name it FAINE, Fast artificial intelligence neutron detection. FAINE uses an artificial neural network of type U-Net and its development consisted with three stages. The first stage is neutrons tracks manual tagging, the second stage is neural network architecture setup and training, and the last stage was evaluating the neural network performance on a test set of neutron track images over CR-39 detectors. These three stages are discussed in detail in the following subsections. The first and third stages were carried out using a designated SW written for the user interface (UI) of the deep learning model as shown in Figure 1.

2.1. Neutron Tracks Manual Tagging. The first stage was the tagging stage, where we picked 23 dosimeters consisting of 230 images and manually tagged all neutron tracks. Then, we used classical image processing algorithms to automatically detect all the objects in the images and match them to the tagged neutron tracks. Inside the 230 images, 23,567 objects were found and 2,615 of them were valid neutron tracks and 20,952 were not. The rules for deciding which signs are valid neutron tracks were taken from the EDL's work instruction for developing CR-39 detectors for evaluation of fast neutrons, which was adopted from Landauer's work instruction. This instruction relies on a worldwide knowledge and experience regarding the neutron tracks morphology. For instance, neutron tracks need to be between certain size limits, they need to have both inner bright circle and outer dark crown and they need to be clear and distinct from their surrounding background. Moreover, they also need to be evenly scattered across the detector area when accumulating large enough statistics. Of course, all the above rules for classifying neutron tracks are somewhat arbitrary, and so is the task of classifying them in every fast neutron dosimetry system. The main important directives to the EDL staff to follow for this classifying task were to obey the above rules and to be as repeatable as a human can be, so the deep learning algorithm described in the next step can learn the neutron tracks features as accurately as possible.

2.2. Neural Network Architecture Setup and Training. For the neutron tracks classification, we chose a state-of-the-art convolutional artificial neural network (ANN) of type U-Net, which was first introduced in 2015 [18] and was fine-tuned later [19]. This network's name is due to both its contracting (downsampling) and expansive (upsampling) paths, which give it the u-shaped architecture (Figure 2). The

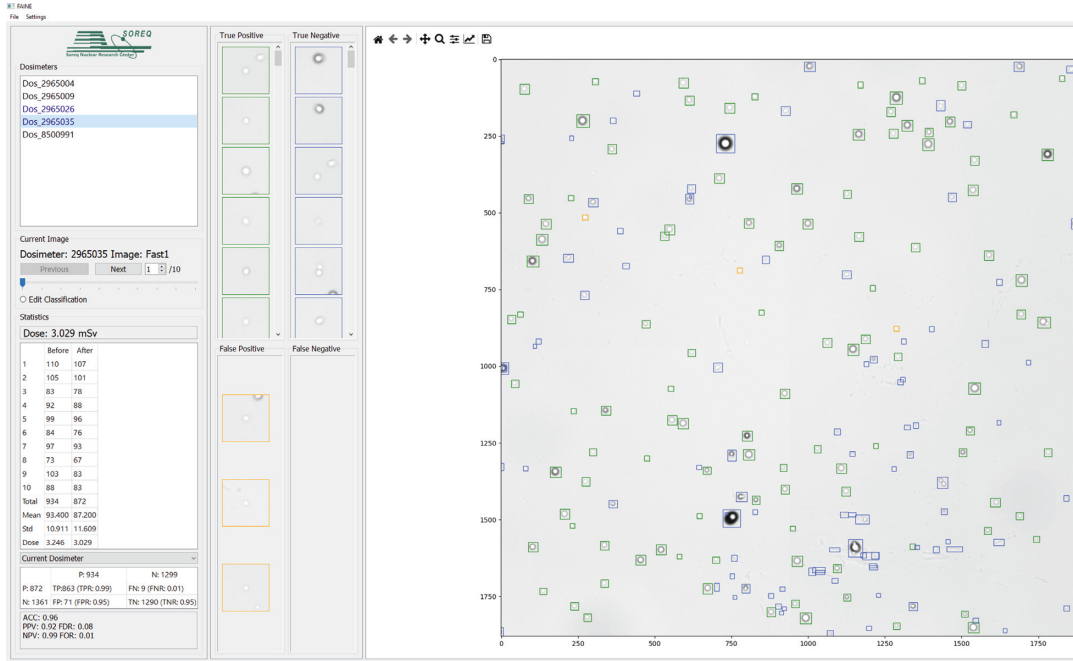


FIGURE 1: An example for the user interface of FAINE. At the large right pane is the 1st out of 10 fields of dosimeter number 2965035 as noted in the upper left pane. At the lower left pane, the statistics of this dosimeter are presented to the user, including predicted vs. real (input) neutron tracks, the confusion matrix, and the algorithm accuracy. In the middle pane, all detected signs are presented in zoom mode, so the user can examine them if needed.

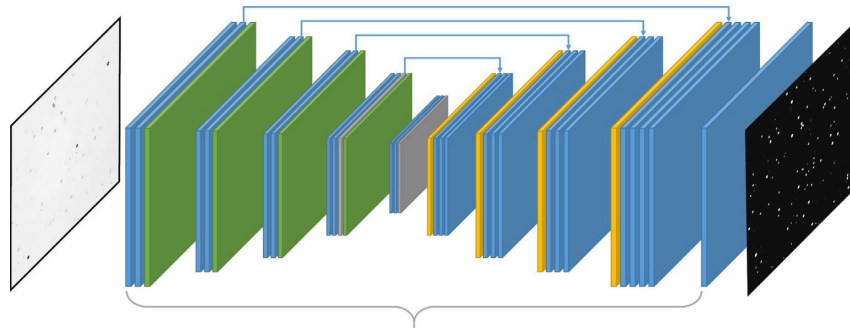


FIGURE 2: Basic schematics of the U-Net architecture. The model input is a raw image and its output is a segmented (masked) image of the neutron tracks. The U-Net consists of a contracting path and an expansive path (encoder-decoder). The contracting path follows the typical architecture of a convolutional network while the expansive path consists of an upsampling of the feature map followed by a 2×2 convolution (“upconvolution”) and two 3×3 convolutions, each followed by a rectified linear activation function (ReLU).

contracting path mainly serves as feature extraction for the net, while the expansive path is more for the localization of objects. U-Net architecture is commonly used for semantic segmentation tasks, e.g., processes of linking each pixel in an image to a class label, in our case either “track” or “nontrack.”

In order to feed the U-Net training stage with good quality images, we used dosimeter images that were taken under different lighting and environment conditions. We then manipulated the data with preprocessing techniques using some classical image processing algorithms such as canny edge detection, dilation, erosion, fill holes, and object detection. For the training stage, we used 80% of the total

23, 567 tagged signs that were created out of the 23 dosimeters, where each image containing such a sign is of resolution of 128×128 pixels.

2.3. *U-Net Performance Evaluation on Neutron Tracks.* After the training stage, we tested the U-Net classifier over the remaining 20% of the 23,567 tagged signs. The metric we used for evaluating the classifier’s performance is accuracy. Accuracy is defined as the number of correct predictions over the number of total predictions, so in terms of a binary classification model as in our case, we have the following definition:



FIGURE 3: An example of FAINE tagging signs inside a CR-39 image. Green squares indicate true positives, blue squares indicate true negatives, red squares indicate false positives, and orange squares indicate false negatives.

$$\text{accuracy} = \frac{TP + TN}{TP + TN + FP + FN}, \quad (1)$$

where TP stands for true positives and is defined as the number of correctly predicted neutron tracks (seen as the track signs inside the green squares in Figure 3), TN stands for true negatives and is defined as the number of correctly predicted signs that are not neutron tracks (seen as the track signs inside the blue squares in Figure 3), FP stands for false positives and is defined as the number of signs that are not neutron tracks, which were falsely predicted as neutron tracks (seen as the track signs inside the red squares in Figure 3), and FN stands for false negatives and is defined as the number of neutron tracks, which were falsely predicted as signs that are not neutron tracks (seen as the track signs inside the orange square in Figure 3).

3. Results and Discussion

As can be seen from Table 1, and using equation (1), when choosing the segmentation threshold to be 0.4, we get an accuracy of 96.7% on our test data.

This accuracy was achieved with respect to 4,509 different tagged signs. We can achieve different true positive

TABLE 1: Confusion matrix of our U-Net model. As can be seen from the definition of accuracy, the two important quantities that contribute to high accuracy are true positives (TP) and true negatives (TN).

Real	Predicted	
		Positives: 1,782
Positives: 1,697	TP: 1,665	FN: 32
Negatives: 2,812	FP: 117	TN: 2,695

Threshold: 0.4.

rate (TPR) to false positive rate (FPR) ratios by applying different classification thresholds over our models prediction. We chose to apply a classification threshold of 0.4 in order to gain a high enough TPR while still maintaining the false negative rates small enough. Of course, this choice of threshold is application-specific, and each model in any scientific field will eventually need to take this choice in order to apply a certain model.

The effectiveness of measuring fast neutron dosimeters at our EDL will dramatically improve, due to the automatic nature of our new tool, which will make the lab technician attendance redundant.

Another advantage of our new tool is the fast neutrons measurement uncertainty expected improvement. Since some of this uncertainty contribution come from the robustness uncertainty, our tool should slightly improve the overall measurement uncertainty by eliminating the worker A vs. worker B robustness term [17].

This measurement uncertainty improvement shall in turn lower the system's detection threshold. The fast neutrons detection threshold is defined in ISO 21909:2015 to be "the minimum measured dose equivalent, which is significantly higher (at the 95% confidence level) than the mean dose equivalent of a sample of nonirradiated detectors." Needless to note that the mean dose equivalent of unirradiated detectors measured by our new tool is supposed to be equal or lower than the one measured by the former method, since the former method used an overshoot dose assessment as a way to address the inherent computer vision problem to detect all fast neutron tracks.

4. Conclusions and Future Work

To conclude, we developed a novel algorithm that uses a deep learning U-Net model to accurately and repeatedly classify fast neutron tracks on CR-39 detectors with a high accuracy of 96.7%. This method can replace manual revision of track counting by an automatic repeatable process that will save a large amount of human time, especially as the number of CR-39 detectors to analyze gets higher in high neutron flux experiments.

It is worth mentioning that such deep learning methods are not limited to detection of massive particles, similar U-Net models can be also used for detection, imaging, and classification tasks with visible, X-ray and gamma photons (see, e.g., [20, 21]) which are now explored at SNRC as well.

In the near future, we plan to extend our U-Net model in order to gain new capabilities for differentiating between alpha-particles and protons and for fast neutrons and alpha-particles spectrometry using machine learning classification. For this extension of our model, we already started a process of its calibration for both alpha-particles detection and for fast neutron spectrometry classification, and we expect that our model will be very useful in analyzing results of proton-boron11 fusion experiments in the future.

Data Availability

The data used to support the findings of this study are available from the corresponding author upon request.

Conflicts of Interest

The authors declare that they have no conflicts of interest.

Authors' Contributions

Both Gal Amit and Idan Mosseri contributed equally to this research and should be considered as co-first authors.

Acknowledgments

This research was funded by the Israeli Ministry of Energy (grant number 01030961) and by the IAEC-UPBC PAZY Foundation (grant number 2472020).

References

- [1] S. Eliezer, H. Hora, J. M. Martinez Val, F. Belloni, and N. Nissim, "Editorial: non-local thermodynamic equilibrium (NLTE) hydrogen-boron fusion," *Frontiers in Physiology*, vol. 8, 2021.
- [2] D. Margarone, J. Bonvalet, L. Giuffrida et al., "In-target proton-boron nuclear fusion using a PW-class laser," *Applied Sciences*, vol. 12, no. 3, p. 1444, 2022.
- [3] S. Eliezer, H. Hora, G. Korn, N. Nissim, and J. M. Martinez Val, "Avalanche proton-boron fusion based on elastic nuclear collisions," *Physics of Plasmas*, vol. 23, no. 5, 2016.
- [4] F. Belloni, "On a fusion chain reaction via suprathermal ions in high-density H-¹¹B plasma," *Plasma Physics and Controlled Fusion*, vol. 63, no. 5, 2021.
- [5] H. Hora, S. Eliezer, G. Kirchhoff et al., "Road map to clean energy using laser beam ignition of boron-hydrogen fusion," *Laser and Particle Beams*, vol. 35, no. 4, pp. 730-740, 2017.
- [6] <https://marvelfusion.com/>.
- [7] <https://hb11.energy/>.
- [8] L. Tommasino, G. Zapparoli, P. Spiezia, R. V. Griffith, and G. Espinosa, "Different etching processes of damage track detectors for personnel neutron dosimetry," *Nuclear Tracks and Radiation Measurements*, vol. 8, pp. 335-339, 1982.
- [9] B. G. Cartwright, E. K. Shirk, and P. B. Price, "A nuclear-track-recording polymer of unique sensitivity and resolution," *Nuclear Instruments and Methods*, vol. 153, no. 2-3, pp. 457-460, Jul. 1978.
- [10] O. P. Massand, H. K. Kundu, M. P. Dhairyawan, and P. K. Marathe, "Studies with CR-39 solid state nuclear track detector for personnel neutron monitoring," *Bull. Radiat. Protect.* vol. 15, p. 27, 1992.
- [11] O. P. Massand, H. K. Kundu, P. K. Marathe, and S. J. Supe, *Development of Neutron Personnel Monitoring System Based on CR-39 Solid State Nuclear Track Detector*, Atomic Energy Commission, India, 1990.
- [12] E. Pitt, A. Scharmann, and R. Simmer, "Model calculations for the fast neutron response of a CR-39 detector covered with a radiator," *International Journal of Radiation Applications and Instrumentation - Part D: Nuclear Tracks and Radiation Measurements*, vol. 19, no. 1-4, pp. 517-520, 1991.
- [13] B. Morelli, E. Vilela, and E. Fantuzzi, "Dosimetric performance of the fast neutron dosimeter for ENEA personal dosimetry service," *Radiation Protection Dosimetry*, vol. 85, no. 1, pp. 105-108, 1999.
- [14] J. Charvat, "Neutron dosimetry based on chemical etching of proton tracks in CR-39," *Radiation Protection Dosimetry*, vol. 23, no. 1-4, pp. 171-174, 1988.
- [15] F. d'Errico, W. G. Alberts, and M. Matzke, "Advances in superheated drop (bubble) detector techniques," *Radiation Protection Dosimetry*, vol. 70, no. 1, pp. 103-108, 1997.
- [16] Y. Eisen, A. Eliaou, and Z. Karpinowitz, "A stable high voltage, high frequency power supply for electrochemical etching," *Nuclear Instruments and Methods*, vol. 174, no. 3, pp. 613-615, 1980.
- [17] G. Amit, O. Even-Hen, O. Awad, Y. Levi, L. Buchbinder, and H. Datz, "A performance study of a new personal neutron

- dosimetry system at SNRC,” *Radiation Protection Dosimetry*, vol. 189, no. 2, pp. 242–252, 2020.
- [18] J. Long, E. Shelhamer, and T. Darrell, “Fully convolutional networks for semantic segmentation,” 2014, <https://arxiv.org/abs/1411.4038>.
- [19] O. Ronneberger, P. Fischer, T. Brox, and U-Net, *Convolutional Networks for Biomedical Image Segmentation*, <https://arxiv.org/abs/1505.04597>, 2015.
- [20] T. Shimobaba, Y. Endo, T. Nishitsuji et al., “Computational ghost imaging using deep learning,” *Optics Communications*, vol. 413, pp. 147–151, 2018.
- [21] T. Bian, Y. Yi, J. Hu, Y. Zhang, Y. Wang, and L. Gao, “A residual-based deep learning approach for ghost imaging,” *Scientific Reports*, vol. 10, p. 12149, 2020.